JOURNAL OF GEOPHYSICAL RESEARCH, VOL. 102, NO. E2, PAGES 3989-4001, FEBRUARY 25, 1997

The Pathfinder Microrover

The Rover Team[1]

Abstract. An exciting scientific component of the Pathfinder mission is the rover, which will act as a mini-field geologist by providing us with access to samples for chemical analyses and close-up images of the Martian surface, performing active experiments to modify the surface and study the results, and exploring the landing site area. Structures, textures, and fabrics revealed in the rover camera images will provide a bounty of geologic information, which can be put in the larger context of geologic features seen in lander camera images. Rover technology experiments will improve our understanding of "soil" properties (grain size, bulk density, friction angle, cohesion, and compressibility) by contributing information not provided by the other Pathfinder instruments. Unplanned opportunities and activities are also likely to provide valuable science information, such as examination of any slumped or eroded soil that has been piled up by the rover wheels, and examination of overturned rocks. Using its ability to actively explore and experiment, the rover will fill in key gaps in our understanding of the landing site.

Introduction

The Microrover (or rover, for brevity) is essential to the achievement of the major scientific goals of the Pathfinder mission because it carries the device (an alpha proton Xray spectrometer, or APXS) that will analyze rocks and other surface materials. Scientific yield will probably be greater than that possible from a fixed platform, like a Viking lander, because of the large area accessible to the rover. The area available to a Viking surface sampler was about 12 m^2 [*Crouch*, 1977], but the area available to the rover is greater than approximately 300 m^2. Scientific contributions of the rover will go well beyond the transportation of the APXS because it is mobile, carries three cameras, and interacts with surface materials. Viking cameras viewed the immediate Martian scenes with high resolution (0.04°/pixel) from fixed platforms, but at large distances, where spatial resolution diminished, exciting landforms could be seen [*Binder et al.*, 1977; *Mutch et al.*, 1977]. The rover could have driven to these landforms and viewed them firsthand and close-up (Figure 1). A wide variety of soil-like materials were sampled and analyzed for inorganic chemical elements by the Viking landers [*Clark et al.*, 1982], but other interesting soil-like materials were beyond the reach of the surface samplers (Figure 2). The rover could have driven to these other materials, examined them, and analyzed their elemental chemistry with the APXS. Rocks were never analyzed by the Viking landers [*Clark et al.*, 1982], but the rover will carry the APXS to rocks for such analyses (Figure 3). This is exciting because the landing site may contain rocks transported by floods from the ancient Martian highlands, younger ridged plains, and other distant units, as well as local volcanic rocks and reworked channel materials [*Golombek et al.*, this issue]. Chemical analyses of such a suite of rocks would provide information on the petrologic and geologic evolution of Mars. The rover will provide great flexibility in the science that can be accomplished; the choices of where to send the rover and what to command the rover to do can be tailored to the actual landing site. There will be other scientific contributions because the wheels of the rover will deform and alter soil-like materials so that their physical-mechanical properties can be estimated, its cameras will view surfaces at higher spatial resolutions than the lander camera, and its cameras will view surfaces that are inaccessible to the lander camera. Depending on the terrain and the location of the lander, the rover might even climb to the rim of a crater and see to greater distances than the lander camera so that locations within the site can be established (Figure 3). The two forward cameras will provide images for stereoscopy and measurements, while the aft camera will provide spectral information. Most, if not all, of the technology experiments that are planned are of scientific interest. Formation of piles of surface materials and excavations by the rover wheels will create topographic configurations and materials that are no longer in equilibrium with the current aeolian environment, so that the chances of detection of erosion by the wind will be increased [e.g., *Arvidson et al.*, 1983; *Moore*, 1985].

[1]Rover core team: J.R. Matijevic, D.B. Bickler, D.F. Braun, H.J. Eisen, L.H. Matthies, A.H. Mishkin, H.W. Stone, L.M. van Nieuwstadt, L.-C.Wen, and B.H. Wilcox (Jet Propulsion Laboratory, California Institute of Technology, Pasadena); D. Ferguson, G.A. Landis, and L. Oberle (NASA Lewis Research Center, Cleveland, Ohio). Rover engineering team: L.W. Avril, R.S. Banes, R.S. Blomquist, G.S. Bolotin, D.R. Burger, B.K. Cooper, F. Deligiannis, W.C. Dias, B.H. Fujiwara, R.D. Galletly, G.S. Hickey, K.A. Jewett, E.J. Jorgensen, H.A. Kubo, W.E. Layman, D.P. McQuarie, R.J. Menke, D.S. Mittman, J.C. Morrison, T.T. Nguyen, D.E. Noon, T.R. Ohm, G.M. Shinn, D.L. Shirley, A.R. Sirota, C.B. Stell, L.F. Sword, H.C. Ta, A.D. Thompson, M.T. Wallace, and Y.C. Wu (Jet Propulsion Laboratory, California Institute of Technology, Pasadena); P. Jenkins, J. Kolecki, and S. Stevenson (NASA Lewis Research Center, Cleveland, Ohio). Contributions by H.J. Moore (U.S. Geological Survey, Menlo Park, California) and J. Crisp (Jet Propulsion Laboratory, California Institute of Technology, Pasadena).

Paper number 96JE01922.
0148-0227/97/96JE-01922$09.00

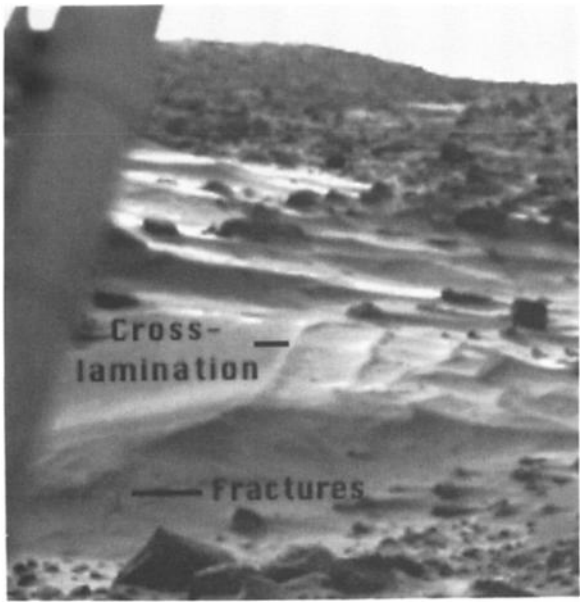

Figure 1. Drifts beyond the sample field and about 10 m from the Mutch Memorial Station (MMS, or Lander 1). Note open fractures and cross laminations. The rover could drive to drifts like these, excavate trenches, examine them, and place the APXS on them for analyses (Viking frame 11H080/582).

Rover missions, objectives, and requirements are not the same as those of the lander. Initially, rover operations will probably be within 10 m or less of the lander. Duration of the Primary Mission is 7 sols (Martian days), and the Primary Mission objectives are (1) exit the lander as early as practical, on the basis of analysis of monochromatic stereoscopic panoramas from the lander camera, (2) send initial vehicle performance and technology experiment data to the lander, (3) move a few meters and send more vehicle performance and technology experiment data to the lander, (4) acquire images showing the condition of the lander and transmit them, (5) acquire images at the end of daily traverses for navigation purposes, or encounter, acquire, and transmit an image or images of a rock or soil patch for subsequent APXS analysis, (6) deploy APXS on a (or the imaged) rock or soil patch for 1 to 10 hours duration (may occur at night) for chemical analysis, (7) query the APXS for final data and transmit interim and final data to the lander, and (8) traverse diverse terrains and send vehicle performance and technology experiment data to the lander. If spacecraft-, rover-, and site-related factors permit, objectives and requirements may be exceeded by deploying the APXS for additional analyses of soils and rocks and the acquisition of more data for the technology experiments. The duration goal of the Extended Mission is 30 sols (Martian days), but a longer duration is possible. Extended Mission objectives are like those of the Primary Mission, but they also include exploration of diverse terrains on Mars well beyond the lander, perhaps as far as a few hundred meters. For example, the rover could go to the elevated rim of an impact crater, view the distant terrain, provide information on its location, and examine and analyze rocks that were once deeply buried (Figure 3).

In this paper, the Rover Team briefly (1) describes the salient characteristics of the rover and its cameras, (2) discusses physical-mechanical properties of surface materials, (3) suggests how some of the physical-mechanical properties may be estimated, (4) discusses structures, fabrics, and textures in rocks and soil-like materials, (5) outlines the technical experiments and their values, and (6) speculates about unplanned opportunities and natural situations where the rover may contribute to our understanding of Mars.

Rover

The rover is carried from Earth to the surface of Mars in a stowed condition on one of the Pathfinder lander petals. After landing, lander-petal deployment, and airbag retraction, the rover and ramps are released by pyrotechnic devices and then the rover rotates its wheels to reach its full dimensions and achieve a deployed configuration. It then drives down the ramps to the Mars surface and begins its mission (Plate 1 and Figure 4). Power is supplied by a solar array backed up by primary batteries. All primary objectives can be accomplished during sunlit hours with a functioning solar panel and dead batteries. Alternately, primary objectives can be accomplished with good batteries and a nonfunctioning solar panel. Rover components not designed to survive ambient Mars temperatures are contained in the warm electronics box. The warm electronics box is insulated with solid silica aerogel and fiberglass walls, coated with low-emissivity films, and heated under computer control. Mass, dimensions, and other characteristics of the rover are given in Table 1.

Six wheels powered by six separate motors (four of these wheels are steerable and powered by four separate motors) and the rocker-bogie system (suspension system without axles or springs) [*Bickler*, 1992] form a versatile rover that can turn around in-place and climb a step with a rise somewhat greater than the diameter of a wheel. Wheel motors deliver torques that greatly exceed those required to move the rover up steep slopes. Because the wheels are separately powered, the rover can rotate some wheels with the

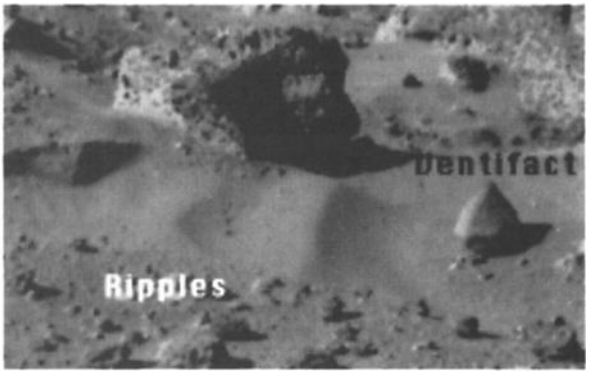

Figure 2. Ripple bedforms about 6.5 m from Lander 2 and 2.5 m beyond the sample field. Are these bedforms composed of granules [*Sharp and Malin*, 1984] or very fine grained drift material [*Moore et al.*, 1987]? Is small pointed rock to right of bedforms a ventifact or a shatter cone? Pointed rock is 0.2 m wide; rock beyond bedforms is 0.7 m wide (Viking frame 22H066/626).

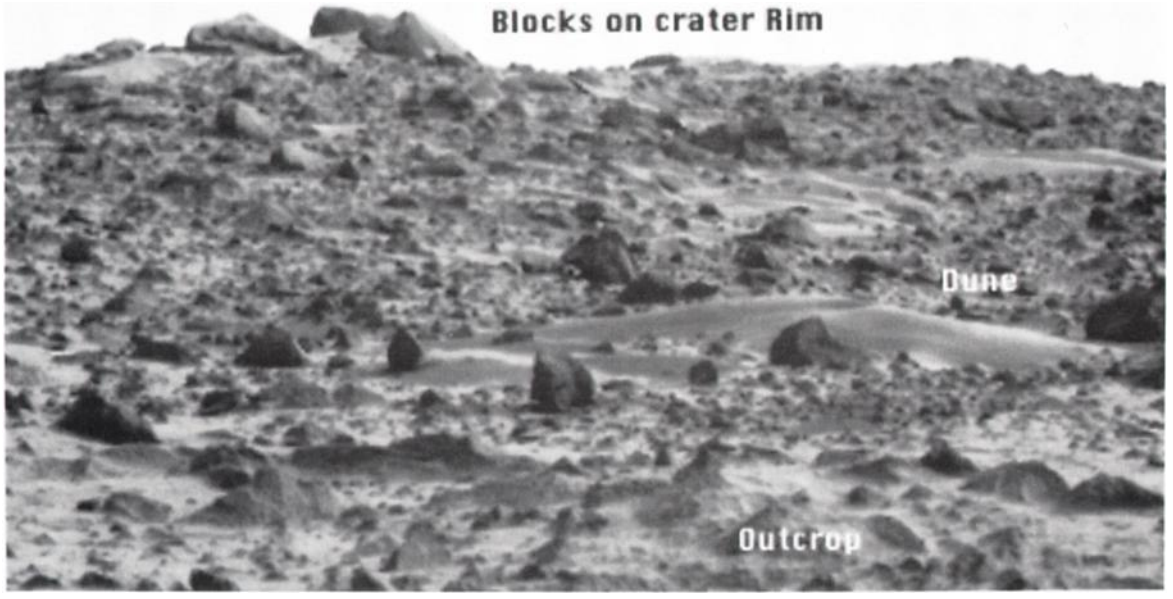

Figure 3. Probable outcrop, possible active sand dune, and rim of impact crater with ejecta blocks nearly 3 m across; distances from the MMS are about 8, 15, and 80 m, respectively; impact crater is about 180 m across and southeast of the MMS [*Morris and Jones*, 1980]. Rover could drive to the outcrop, dune, and crater rim, examine them, and place the APXS on the materials for analyses. Materials excavated from the greatest depths are found on rims of impact craters. Rover views from elevated crater rim would extend to distances beyond those of the lander cameras and would permit location of the rim by resection (Viking frame 12C184/246).

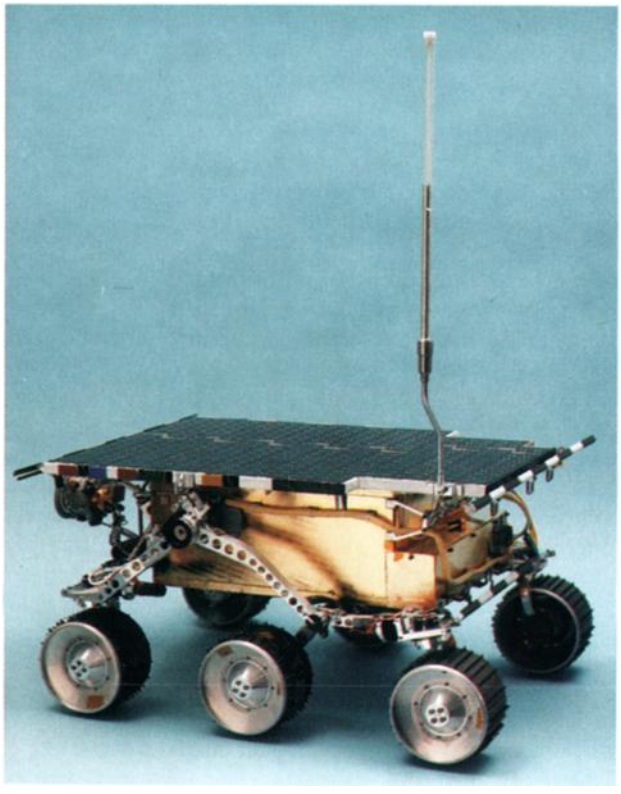

Plate 1. Oblique color photograph of the rover (see Figure 4).

others locked so that a variety of tasks using the wheels can be accomplished. Among the tasks are wheel spinning, skidding, plowing, and trenching. In the unlikely event that the landing site is contaminated by materials from the descent rocket exhausts or airbags (Al_2O_3, NH_4Cl, and C soot), the rover may be able to locate rock faces that are uncontaminated and excavate to expose fresh soil-like materials.

There are three cameras aboard the rover. Two broadband monochrome cameras are located on the forward part of the rover. A third camera is located on the aft part of the rover near the APXS. The aft camera has a pixel array that allows imaging in three colors, yielding some information on the surface materials. For every 4×4 block of 16 pixels on this color camera, 12 are green, two are red, and two are infrared. Spectral response of the camera for each of the three types of pixels is shown in Figure 5. The response of the infrared pixels is low, compared to that for the red and green. Unfortunately, increasing the exposure time to improve the dynamic range of the infrared pixels results in bleeding of light from the red and green pixels into the infrared pixels. Thus the color camera will primarily be useful only for red and green color information. Color calibration patches along the edge of the solar panel (see Plate 1 and Figure 4) will be used to corroborate spectral calibration of the lander camera, and images of the same patch of soil or rock by both the lander and the aft rover cameras will allow calibration of the spectral response of the aft rover camera. Furthermore, similar calibration targets are mounted on the rear rover ramp, allowing a predeployment

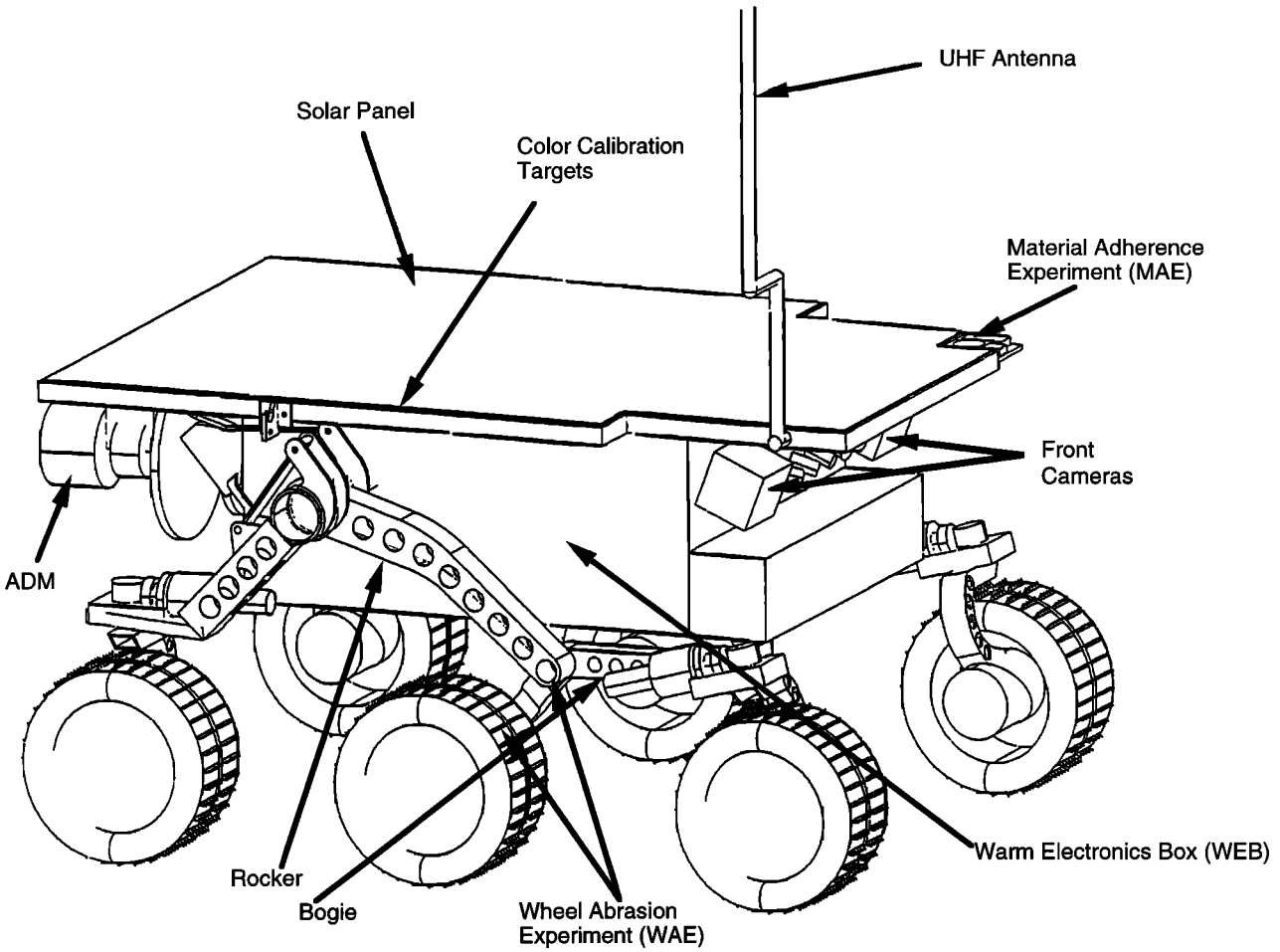

Figure 4. Sketch of the rover, highlighting features seen in Plate 1; solar panel with color calibration targets along the edge, rocker-bogie suspension system, wheels, front cameras, UHF antenna, warm electronics box, material adherence experiment, wheel abrasion experiment, and APXS deployment mechanism.

calibration of the rover color camera. Although the lander camera has much better spectral resolution than the rover color camera, the rover camera images will have better spatial resolution under some conditions. (Spatial resolution is the product of the distance of an object or surface from the camera and the camera resolution in mrad/pixel.) The forward cameras will provide stereoscopic information on surface configurations at fine scales. Characteristics of the cameras are given in Table 2.

Vehicle control is provided by an integrated set of computing and power distribution electronics. The computer performs input/output to about 70 sensor channels, and it services such devices as the cameras, motors, and experiment electronics. Motion control is accomplished through the on/off switching of the drive or steering motors. An average of motor encoder (drive) or potentiometer (steering) readings determines when to switch off the motors. When motors are off, the computer conducts a proximity and hazard detection function, using its laser striping and camera system to determine the presence of obstacles in its path. The vehicle is steered autonomously to avoid obstacles but continues to seek the commanded location. While stopped, the computer also updates its measurement of distance traveled and heading using the average of the number of turns of the wheel motors and an onboard gyroscope. This provides an estimate of progress to the commanded location and distance to the lander.

Command and telemetry are provided by UHF radio modems on the rover and lander. During the day, the rover will regularly request transmission of any commands sent from Earth and stored on the lander. This request will typically be made at about 10-min intervals during the day and every hour or two at night when APXS measurements are taken. When commands are not available, the rover transmits any telemetry collected during the last interval between communication sessions. The telemetry received by the lander is stored and forwarded to Earth. In addition, the communication system is used to provide a "heartbeat" signal during vehicle driving. While stopped, the rover sends a signal to the lander. Once acknowledged by the lander, the rover proceeds to the next stopping point along its traverse. If the heartbeat is not acknowledged, the rover will back up to attempt to reestablish communication.

Commands for the rover are generated, and analysis of telemetry is performed at the rover control workstation, which is a Silicon Graphics computer and a part of the Mars Pathfinder ground control operation. At the end of each sol of rover traverse, the lander camera takes a stereo image of

Table 1. Rover Characteristics

Parameter	Value
Deployed Dimensions, cm	
Length	62
Width	47
Height	32
Rover and Payload	
Mass	10.5 kg
Approximate weight on Mars	38.8 N
Nominal Mass Per Wheel Pair, kg	
Front	(27%) 2.8
Middle	(36%) 3.8
Rear	(37%) 3.9
Speed	
Nominal	0.4 m/min
Rough terrain	0.25 m/min
Turning	7 deg/s
Wheels (Six), cm	
Diameter	13
Width	6
Array Power (13 Strings of 18 5.5-mil GaAs Cells), W	
Peak power at noon, array alone	15.8
Peak power at noon, battery and array at 9 V	30
Energy Storage (3 Strings of 3 LiThCl Cells)	
Beginning of life	150 W h
Power Drawn by the Rover[a], W	
Nominal, at -40 °C	7.6
Nominal, at -80 °C	13.3
Rough terrain, at -40 °C	8.4
Rough terrain, at -80 °C	13.9

[a]These values were derived on the basis of the rover driving, so these power numbers include the CPU, input/output, gyroscope, encoders, and accelerometers powered as well as the motors. Nominal driving is defined as "6 motors powered no load," which is consistent with coasting on flat terrain. Rough terrain driving is defined as "two motors at 1 N m each, two motors at 0.5 N m each, and two motors at no load," which is consistent with the rover climbing. As such, a motor at 1 N m torque output is applying a force of 15.4 N at 0.065 m (a wheel radius). Thus two motors at 1 N m torque produce 30.8 N, and two motors at 0.5 N m torque produce 15.4 N for a total of 46.2 N. The rover at delivery is 10.5 kg, so it weighs 38.6 N on Mars. Thus (with 7 N of margin) the rough terrain driving shows the power needed to climb a step (lifting the rover straight up). The stall torque (torque that will cause the motor to stop) for a given motor ranges from 8.2 N m at 0°C to 12.4 N m at -80°C. This says that the motors have the capability to apply from 8 to 12 times more torque per wheel. The only constraint is power available to supply these motors. At -80°C, a motor at stall draws 255 mA at 15.5 V. At 0°C, a motor at stall draws 196 mA at 15.5 V.

the vehicle in the terrain. Those images, portions of a terrain panorama, and supporting images from the rover cameras are displayed at the control station. The operator is able to designate points in the terrain on the displayed images. These points serve as target locations for rover traverses. In addition, the operator can use a model of the vehicle which, when overlaid on the image of the vehicle, measures location and heading. This information is transferred into the command file to be sent to the rover on the next sol to direct the rover to the new target locations and correct any navigation errors.

The APXS deployment mechanism (ADM) is mounted on the rear of the rover and will allow placement of the APXS sensor head against rocks and soil-like materials for analyses [see also *Blomquist*, 1995; *Rieder et al.*, this issue]. The rover must be azimuthally positioned and aligned to place the sensor head on a given sample site because the mechanism moves the head along a fixed path with respect to the rover until the head contacts a surface. This fixed path forms an arc from the stowed position on the rover to the surface in the plane of bilateral symmetry of the rover. Its flexible wrist and motor-driven parallel-link arm align the head to within 20° of surfaces on rocks as high as 29 cm and on soil as low as 5 cm below the bottom of the rover rear wheels. The ADM can be deployed to surfaces tilted as much as 45° from the nominal orientation of the sensor head face, which ranges from vertical for a high rock to horizontal for a flat soil. When the ADM bumper ring is placed against a solid surface, the APXS sensor head detectors are 5 cm away from the surface, inside a cylindrical ring behind the bumper. Penetration of the ring into a soil-like material will reduce this distance. The signals from three pairs of light-emitting diodes and phototransistors, on spring-loaded plungers behind the bumper, will provide feedback to the rover to indicate when to stop the moving ADM as it is being positioned against the surface with forces typically between 0.5 and 3.0 N.

Times required for the placement of the APXS sensor head on rocks and soil-like materials will vary because of mission- and landing-site-related factors. If no rover movements are required, the ADM can place the sensor head on a soil-like surface within a minute or so. In contrast, a longer time would be required for a local exposure of crust if the rover must traverse to the local exposure and position itself in such a way that the ADM will place the sensor head on the crust. Similarly, the rover must traverse to the vicinity of a rock and then position itself at the proper distance and with the proper alignment for placement of the sensor head on a surface of the rock. Nominally, final placement of the ADM may be accomplished within about 5 min when the rover is near a rock by deploying the sensor head to a specified position, turning the rear of the rover toward the rock,

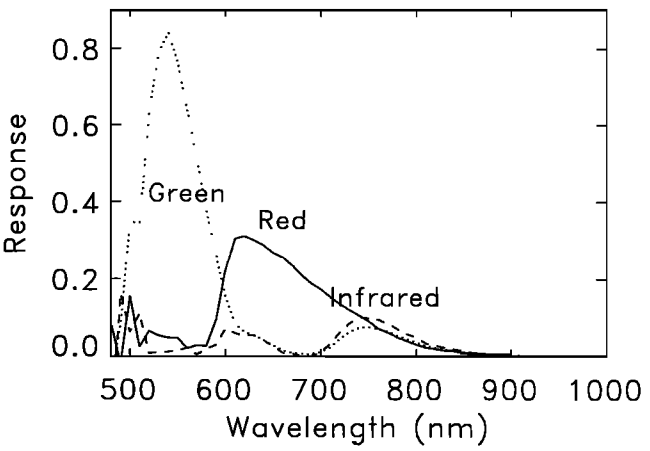

Figure 5. Relative spectral response of the rover color camera, for the green, red, and infrared pixels. ZnSe optics in the camera lens cuts off all light at wavelengths shorter than 500 nm.

Table 2. Camera Characteristics: Two Forward and One Aft

Parameter	Value
General Camera Features	
Charge coupled device array size	768 × 484 pixels
Lens focal length	4 mm
Forward camera separation	12.56 cm
Approximate height above surface	26 cm
Fields of View, deg	
Forward	127.5 (cross track)
	94.5 (along track)
Aft	94.5 (cross track)
	127.5 (along track)
Resolutions[a]*, mrad, deg*	
Forward	2.897, 0.166 (cross track)
	3.409, 0.195 (along track)
Aft	3.409, 0.195 (cross track)
	2.897, 0.166 (along track)
Boresight Angle, deg	
Forward	-22.5
Aft	-41.4
Wavelength Sensitivity, nm	
Forward	830-890
Aft	see Figure 5

[a]Average spatial resolution per pixel is 0.003153 times the distance from camera.

and backing toward the rock until contact of the sensor head actuates an ADM switch that stops the rover. The sensor can also be placed on a rock in a fashion similar to that used for soil-like materials. Placement of the sensor head on dust-free parts of rocks may take a considerable, but unknown, amount of time because multiple command cycles may be necessary to meet very stringent positioning requirements for small target areas. Successful deployments are contingent on an accurate knowledge of the locations of materials in the site and rover characteristics.

Surface Materials

A primary goal of the Rover Team is to understand the physical-mechanical properties of the surface materials, their topographic expressions, and their abundances, because they are important factors that affect rover mobility and surface operations. These same factors are of scientific importance because they control the responses of the materials to geologic processes, are the result of past and current geologic processes, and produce the bulk remote-sensing signatures of the landing site. In this section, we briefly review some physical-mechanical properties of natural materials. Other topics are discussed in subsequent sections.

The physical-mechanical properties of interest are grain characteristics (size, distribution of sizes, shape, etc.), density, friction angle, cohesion, and compressibility. Soil-like materials and rocks are composed of rock, mineral, and/or mineraloid grains that are held together by interparticle forces or by cementing substances with pore spaces between the grains. The grain size of a material may range from micrometer to dekameter sizes. The grains may be well sorted, as in some sands, or poorly sorted, as in ejecta from impact craters; they may be rounded, as in stream cobbles, or angular, as in talus. When the interparticle forces are negligible and cementation absent, the material is cohesionless, as in dry beach sand. When aggregates of small grains are held together by moderate interparticle forces with various magnitudes or cements, cohesive clods of various strengths and sizes are formed, as in garden and natural soils. Similarly, rocks are made of grains held together by strong forces and, often, with very little pore space between the grains. Density is the mass of a material per unit volume. In the case of natural materials, the term bulk density is used because they are usually made of grains and/or rock fragments with different densities and variable amounts of pore space between the grains and fragments. For example, a rock composed of mineral grains that have densities of 2600 to 3000 kg/m^3 may have a bulk density of 2700 kg/m^3. When the rock is broken into fragments and poured into a container, new open spaces or pores are formed between the rock fragments and the resulting bulk density could be about 1600 to 1700 kg/m^3. Porosity and void ratio are quantities related to grain and bulk densities. Porosity is the volume fraction of pores in the material, and void ratio is the ratio of the volume of pores and solid grains [e.g., *Hough*, 1957, p. 32]. Cohesion and friction angle are parameters that describe the strength of rocks and soil-like materials. The criteria for mechanical failure of these materials may be described by the Mohr-Coulomb law [*Terzaghi*, 1948]:

$$T = T_o + (S - P) \tan \phi, \quad (1)$$

where T is the shear stress parallel to the plane of failure, T_o is the cohesion, S is the stress normal to the plane of failure, P is the pore pressure, and ϕ is the friction angle. Tan ϕ is the coefficient of friction. Cohesion is related to cementation and forces between the grains and fragments of the material. Pore pressure effects (P) for the rover on Mars are probably negligible because the rover moves slowly and the atmospheric pressure at the surface of Mars is around 700 Pa. Compressibility is the relation between applied load and void ratio [see *Hough*, 1957, pp. 97-121] and is a function of the initial properties and history of the material. For soil-like materials, the mechanical properties may be interrelated. *Mitchell et al.* [1972] found that the coefficient of friction and cohesion of their lunar surface simulant (ground basalt) increase with increasing bulk density.

To a first order, we expect that the surface materials on Mars will be like those on Earth [e.g., *Moore et al.*, 1982, 1987]. On Earth, rocks, such as dense basalts and granites, commonly have bulk densities near 2500 to 2900 kg/m^3, friction angles near 40° to 60°, and cohesions that are measured in MPa; they are incompressible for practical purposes. Cohesive soil-like materials commonly have bulk densities near 1200 to 1800 kg/m^3, friction angles near 25° to 40°, and cohesions that are measured in kPa and fractions of a kPa; they are compressible; small friction angles are possible when bulk densities are small. Sands commonly have bulk densities near 1700 kg/m^3, friction angles near 34° to 45°, and moderate compressibilities (sand may dilate when deformed). Loose, dry sand is cohesionless, but sand may have a shear strength intercept, analogous to cohesion, that is a function of the grain size of the sand [*Seed and Goodman*, 1964].

Estimating Physical-Mechanical Properties

In this section, Viking and lunar experience will be used to illustrate possible ways to estimate some physical-mechanical properties. The use of the rover and lander cameras is essential to achieving these estimates. These estimates will not be refined and extensive like those for the lunar regolith [*Carrier et al.*, 1991] because a host of tools and instruments is not available and no samples will be returned to Earth, but preliminary tests with a lunar regolith simulant suggest that good estimates of friction and cohesion will be obtained using rotations of the rover wheel. The large forces available for the Viking sampler soil tests (about 223 N) on Mars will not be available to the rover, but similar tests at shallower depths may be possible. Important is the fact that, because of its mobility, the rover might establish the presence of more types of soil-like materials than Viking. Lander 1 penetrated and tested two very different types of soil-like materials [e.g., *Christensen and Moore*, 1992], and there may be others.

Grain sizes. There are no instruments aboard Pathfinder that are specifically designed to measure grain size, but much of the information will come from the rover and lander cameras. In particular, sizes and shapes of grains, fragments, and rocks can be determined by direct viewing if they are large enough. In order to fully resolve clods, grains, and fragments in the images, experience has shown that they must be about 3 to 5 times larger than the spatial resolution of the camera. With these criteria, the lander camera (1 mrad or 0.057° resolution per pixel) should be able to fully resolve fragments 0.68 to 1.1 cm across at a range of 2.26 m and 3 to 5 cm across at 10 m. The rover cameras should be able to resolve fragments about 0.6 to 1.0 cm across at a nominal range of 0.65 m, but closer viewing of the surface near the wheels could reduce these sizes by four-tenths, and special situations (such as close-up views of a rock 20 cm high) could reduce these values by as much as one-tenth. Comparison of Figures 6 and 7 demonstrates the improved clarity of rock roughness and texture at a distance of 25 cm (0.8 mm/pixel spatial resolution) over that at 40 cm (1.2 mm/pixel spatial resolution). Interpretations and measurements will be enhanced by stereoscopic viewing, measurements, and spectral information.

Viking showed that the soil-like materials sampled by the Gas Exchange Experiment had specific surfaces consistent with grain sizes near a few micrometers [*Oyama and Berdahl*, 1977; *Ballou et al.*, 1978], but physical sizes could have been near 10 μm [*Moore and Jakosky*, 1989]. This size is much too small to view directly with the lander and rover cameras. However, constraints can be placed on the grain size by observing how the materials react to the wheels of the rover and the bumper of the APXS deployment mechanism. Tracks in poorly sorted compacted sand exhibit tread marks that are difficult to see with the rover camera (Figure 8, left). Dry beach sands will form V-shaped ruts with elevated rims and surfaces that appear dull and diffuse in the images. In contrast, compressible soil-like materials composed chiefly of silt- and clay-size grains will form ruts with steep walls that contain smooth, reflective areas of compacted material (Figure 8, right). The grain size of the lunar regolith was constrained in this way during the unmanned Surveyor Lander Program [*Christensen et al.*, 1967], and Viking reaffirms the validity of the approach [*Moore et al.*, 1987]. The deployment of the APXS onto the surface will produce indentations that can be interpreted in similar ways (Figure 9).

Bulk density. Like grain size, there is no Pathfinder instrument specifically designed to measure densities. Grain densities might be estimated on the basis of mineralogies inferred from APXS chemical analyses. Bulk densities

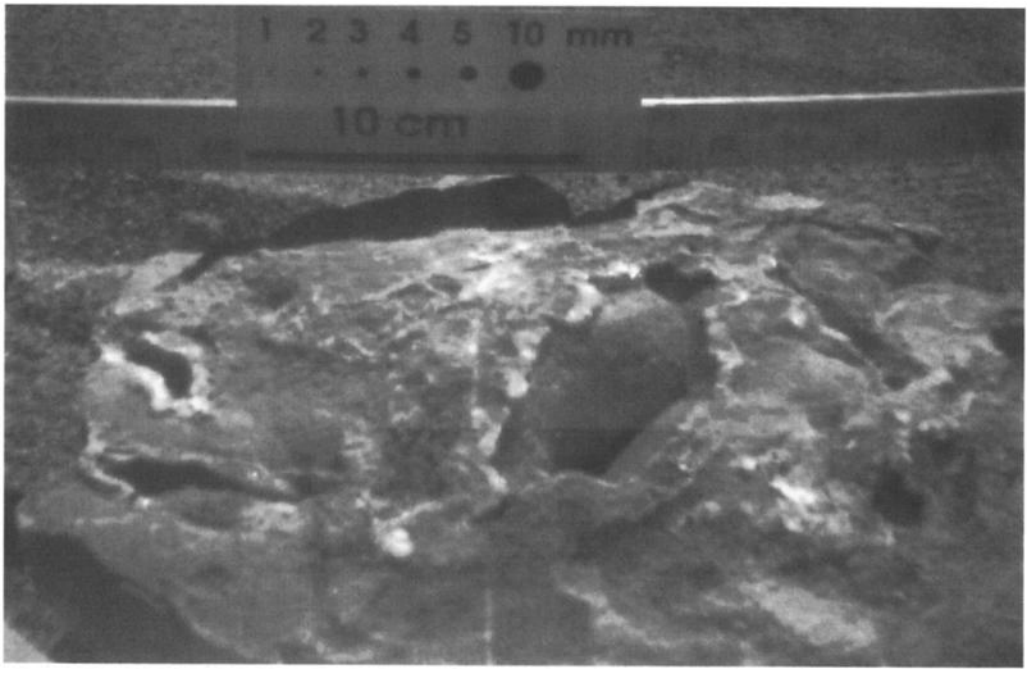

Figure 6. Left front rover camera view of sedimetary rock surface with crystal-lined vugs, taken from 25 cm (381 × 248 pixel subframe). This image is made up of three horizontal segments, each taken with its own autoexposure time, to limit dark current noise (which will not be a problem at Mars temperatures).

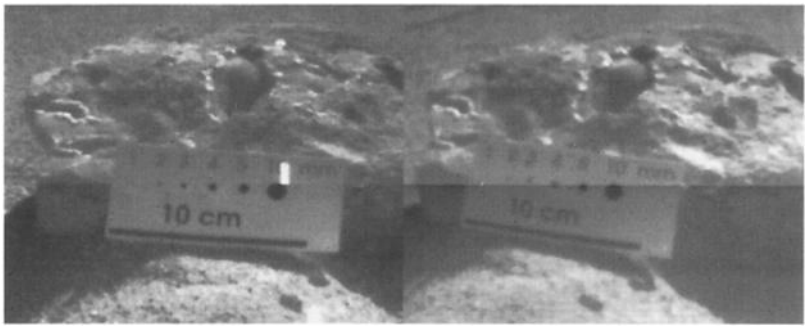

Figure 7. Stereoscopic pair of same rock shown in Figure 6, from 40 cm taken with the forward cameras of the rover (two 214 × 173 pixel subframes). Each image is made up of three horizontal segments with separate autoexposure times. White spots are CCD blooming artifacts. The biggest coarse sand grains are nearly resolved. A couple of centimeter-size rocks are in the foreground.

pose different problems because porosities, as well as grain densities, must be known. Bulk densities inferred for rocks might be reasonable because their porosities tend to be low and inspection of them could provide an estimate of porosity. Soil-like materials are another matter because they are often fine-grained and porous. However, bulk densities of soil-like materials might be constrained because their friction angles tend to correlate directly with bulk density [*Mitchell et al.*, 1972]; moderately dense soil-like materials have friction angles near 30-40°, whereas low-density soil-like materials have smaller friction angles.

Friction angle. Friction angle might be estimated in two ways. In the first, simultaneous solutions of the Mohr-Coulomb equation for friction angle (and cohesion) using forces or stresses derived from wheel torques for two or more loading conditions might be used (see subsection on basic soil mechanics under the section on technology experiments). For Viking, plowing theory [*McKyes and Ali*, 1977] was applied to the geometry of sample trenches and surface deformations in front of the sampler to estimate friction angles with reasonable results [*Moore et al.*, 1982, 1987] (Figure 10). Analogous experiments may be possible with the rover, but forces exerted on the materials will normally be limited by the rover weight and the properties of the materials. Expected motor torques are listed in Table 1, and the measurement resolution will be of the order of 0.2 N m or better. Like Viking, the lander and rover cameras provide the image pairs for stereometric measurements of experimental conditions and surface deformations.

Cohesion. Like friction angle, cohesion can be also obtained by simultaneous solutions of the Mohr-Coulomb equation using forces estimated from wheel torques and images for two or more loading conditions. In a second method, wheel torques are combined with the friction angle using plowing theory [*McKyes and Ali*, 1977] to calculate cohesion [*Moore et al.*, 1982, 1987]. Again, forces will normally be constrained by the weight of the rover and the materials.

Compressibility. Compressible materials are found at the surfaces of the Earth's moon and Mars. For the Moon, this is illustrated by astronaut bootprints [*Scott et al.*, 1970], and for Mars, by rimless pits produced by the impact of engine exhaust debris in drift material. The rover, with a mass of 10.5 kg, will weigh about 39 N and exert stresses near 2 kPa when forces are allotted equally to each wheel with a bearing area near 6 cm on an edge; 2 kPa is about 0.3 times load on an astronaut boot on the Moon [*Costes et al.*, 1969].

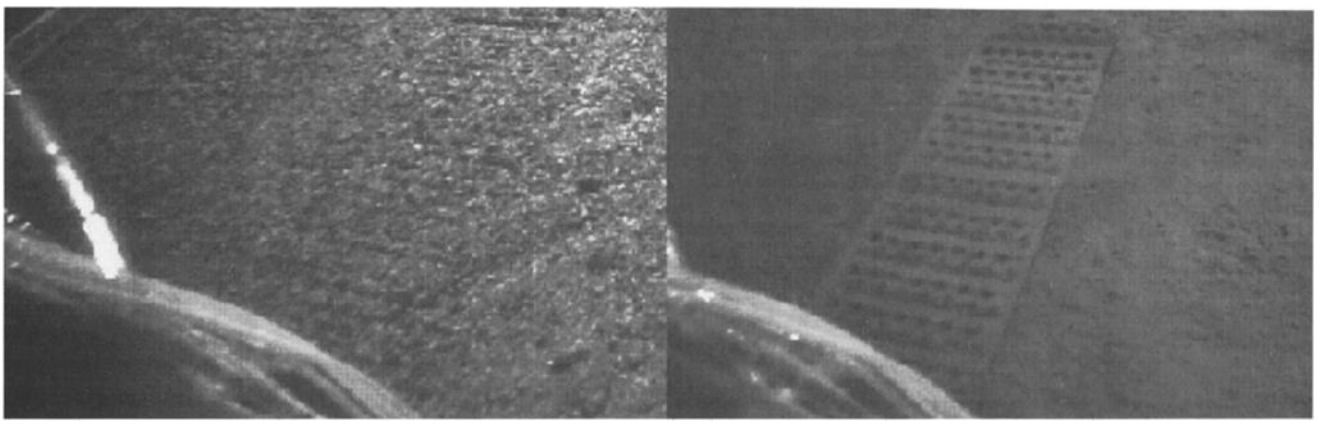

Figure 8. Rover tracks in poorly sorted, well-compacted sand (left image) and fine-grained, loose lunar-like material (right image), as viewed by the left front rover camera (300 × 190 pixel subframes). Each image is made up of two horizontal segments with separate autoexposure times.

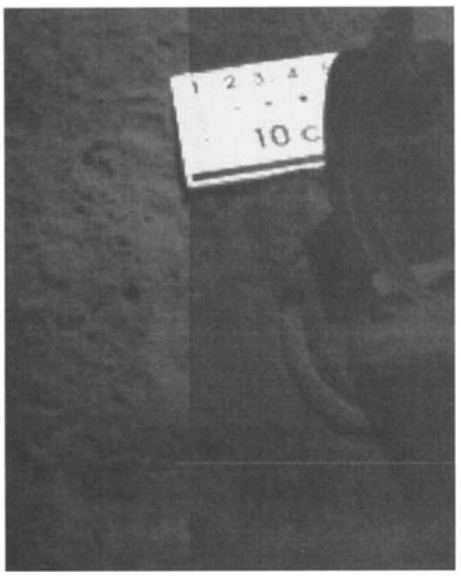

Figure 9. Rear rover camera image of the bumper-ring impression in lunar-like material, after deployment and retraction of the deployment mechanism for the alpha proton Xray spectrometer (APXS) (170 × 250 pixel subframe). Although the flight rover will have a color rear camera, this image was aquired with the flight spare rover using a monochrome version of the rear color camera. Scale bar is the same as shown in Figure 6. Some of the impression is obscured by the rover itself, but this image shows the scene viewed by the rear camera after retracting the APXS deployment mechanism without moving the rover. Each image is made up of two vertical segments with separate autoexposure times.

Structures, Textures, and Fabrics of Rocks and Soil-Like Materials

Observations of rocks, close-up, offer exciting possibilities for making new discoveries about Mars because structures, textures, and fabrics will provide information on the geologic histories of the rocks [e.g., *Lahee*, 1941; *Compton*, 1962; *Shoemaker et al.*, 1969], landing site, and Mars. Structures, such as vesicles, bands, laminations, fractures, and joints in igneous rocks and vugs, bedding, layers, open fractures, and joints in sedimentary rocks, may be visible (e.g., Figure 6). Angles between the shear fractures in rocks could be measured using stereometry and friction angles inferred from them. Similarly, the open fractures in drifts, cross laminations in drifts and dunes, and layers of crust in soil-like materials, like those observed by the Viking landers, could be inspected in detail. Observations will be enhanced by stereoscopic viewing (Figure 7) and spectral information. The potential for interpreting structures, fabrics, and textures of rocks with rover images is illustrated with Figures 6 and 7, which show a sedimentary rock that contains vugs lined with a white mineral. An image taken from 25 cm with a resolution of 0.8 mm/pixel clearly reveals the white linings of the vugs and their thicknesses can be measured (Figure 6). Stereoscopic viewing of an image pair of the same rock from 40 cm shows the details of the topography of the surface of the rock and that the vugs are, in fact, depressions (Figure 7). Inspection of the stereoscopic images also reveals the topography and presence of coarse grains in the piles of poorly sorted sand below the scale in Figure 7. Although untested, stereometric measurements may provide accurate values for slopes and relief of similar piles. For the stereoscopic images (Figure 7), the resolution is 1.2 mm/pixel. The combination of 1.2-mm resolution and stereoscopic viewing offers the possibility of recognizing very coarse grained and porphyritic igneous rocks, breccias, conglomerates, coarse-grained sandstones, and a host of other textures [*Lahee*, 1941; *Compton*, 1962]. In some cases, fabrics such as crystallinity or packing schemes may be recognizable. Inferences about minerals from color, crystal shape, and cleavage might even be possible for large euhedral crystals, especially when the chemical composition of the host is known. If large crystals or centimeter-size clasts are discernible and chemical compositions are known, comparisons could be made with the Antarctic orthopyroxenite meteorite (ALH84001) or other coarse-grained meteorites that originated on Mars [*Mittlefehldt*, 1994; *Treiman*, 1995]. Viable mineralogic inferences were made for lunar rocks using monoscopic Surveyor images and compositions [*Shoemaker et al.*, 1969], but without the benefit of spectral information. For volcanic rocks, textures and mineralogical constraints could disclose information about the crystallization history and the nature of the eruption. Recognition of a sedimentary rock on Mars would have important implications for paleoclimate and potential fossil life, and this could be done with the rover cameras. Close-up views of rocks could be achieved by placing the cameras near vertical rock faces, and close-up views of soil-like materials could be achieved by digging into the materials to lower the cameras toward the surface. Excavations by the rover also offer a way to examine layers and crusts in soil-like materials.

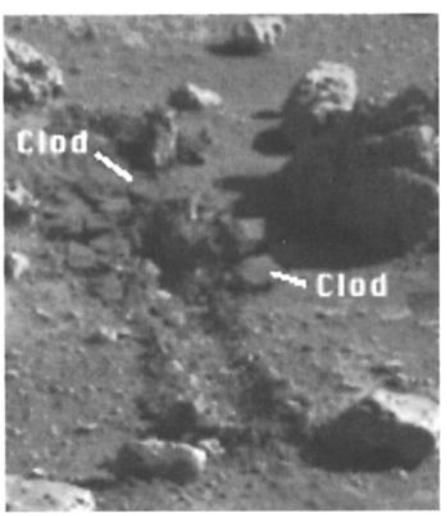

Figure 10. Trench excavated by sampler of Viking Lander 2. Note prismatic clods of deformed cloddy material. Rover may produce similar deformations of surface materials. Trench is about 7 cm wide (Viking frame 21C044/057).

Technology Experiments

Most of the technology experiments will make substantial contributions to the science objectives of the Pathfinder Mission either directly or indirectly. There are 10 technology experiments: (1) terrain characterization, (2) basic soil mechanics, (3) sinkage in each soil type, (4) wheel abrasion, (5) material adherence, (6) thermal characterization, (7) UHF link effectiveness, (8) vehicle performance, (9) dead reckoning and path reconstruction, and (10) vision sensor performance.

Terrain characterization (L. Matthies, B. Wilcox). The objective of this experiment is to determine terrain feature classes (soils, rocks, hills, etc.) as well as statistical size and location distributions of the feature classes using rover and lander camera images. Although oriented toward rover operations, the results from this experiment will be of extreme scientific interest because areal distributions and topographic configurations of soils, rocks, hills, etc. partly control the responses of the surface materials to geologic processes, reflect past and current geologic conditions on Mars, and are responsible for the bulk remote sensing signatures of the landing site.

Basic soil mechanics and sinkage in each soil type (D. Bickler, H. Eisen). This experiment will evaluate the mechanical properties of the Martian surface materials (such as soil energy loss, shear strength, sinkage, shear strength as a function of sinkage, adhesion, and abrasion) using the results of the vehicle performance experiment and rover and lander camera images. Experimental techniques include measuring vehicle performance (motor torque, bogie positions, etc.) during traverses and special experiments. One such experiment will involve rotating one wheel while others are held fixed, and deriving soil shear force from the measurements. Other experiments will likely include some "plowing" or "dragging." Sinkage will be obtained from lander camera images of rover tracks and material abrasion wheel patches and from rover images of a wheel in the soil. Deployments of the APXS to the soil will also leave ring-shaped marks in the soil, which can be studied with rover and lander camera images.

Like the previous experiment, results from this experiment have great scientific value because the mechanical properties of the surface materials partly control the response of the surface to geologic processes, are the results of recent and past geologic processes, and produce the remote sensing signatures of the site. During the wheel rotation experiments, the wheels will dig into the surface materials and may expose layers and crusts.

Wheel abrasion (D. Ferguson, J. Kolecki, S. Stevenson). This experiment will assess abrasive wear on a rover wheel using thin films of Al, Ni, and Pt (200 Å - 1000 Å) deposited on black, anodized Al strips that are attached to the rover wheel (location shown in Figure 4). As the rover moves across the Martian surface, a photocell will monitor changes in film reflectivity. These changes will indicate the amount of abrasion of the metal films by Martian surface materials. Data on wear will be accumulated. In a special experiment, all of the rover wheels will locked to hold the rover stationary while the test wheel is rotated and digs into the surface in order to provide more severe conditions than simple rolling. Laboratory experiments using terrestrial materials and a rover wheel will be used to evaluate the results.

Results will contribute to our knowledge of the surface materials. Marked abrasion will indicate materials composed of hard, possibly sharply edged grains. Lack of abrasion would suggest soft materials. Such knowledge may place constraints on the mineralogy of the soil-like material and contribute to an understanding of erosion processes on Mars.

Material adherence (G. Landis, L. Oberle, S. Stevenson). The goal of this experiment is to measure the change in performance of the solar array caused by dust deposition on the array [*Landis et al.*, 1995]. The experiment employs a reference solar cell with a memory-metal actuated transparent dust cover (location on the rover shown in Figure 4). The actuation mechanism uses the heat-induced phase transformation of Nitinol memory-metal [*Gisser et al.*, 1994] to contract a wire to rotate the cover away from the cell. Comparison of the output of the reference solar cell with and without the transparent dust cover will be a measure of the degradation of the array due to dust deposition. The expected obscuration, at an optical depth of 1, is 0.2% per day [*Landis*, 1994]. Optical depth is a measure of the attenuation of visible light through the atmosphere. The actual obscuration will be proportional to the amount of dust in the atmosphere. Adjacent to the transparent dust cover, the quartz crystal monitor provides a measure of the mass of dust deposited. The exposed surface is coated with a thin adhesive layer to promote adherence of dust to the surface. The oscillation frequency of the quartz crystal changes as mass is deposited on its surface. The sensitivity is 4×10^{-12} kg/cm^2 with 10^{-11} kg/cm^2 instrument drift. Expected atmospheric dust deposition (1.7×10^{-9} to 5×10^{-9} kg/cm^2/d) is well above the sensitivity and drift. Maximum loading is about 1.8×10^{-7} kg/cm^2 and corresponds to 35 days of operation for a rate of dust deposition of 5×10^{-9} kg/d.

These direct measurements of dust deposition will provide valuable constraints on dust accumulation and transport near the surface. Such measurements are needed to improve our understanding of the exchange of dust between the atmosphere and surface of Mars. Separation of dust deposition from rover operations and the atmosphere may be difficult, however. If much of the dust measured by this experiment is kicked up by rover wheels, then it will provide information about near-surface saltation and the nature and distribution of the local fines in the surface material. These results, combined with observations made by the Pathfinder lander camera and estimates of bulk densities of the deposited dust, may help constrain the grain sizes of the dust particles collected on the material adherence experiment.

Thermal characterization (D. Braun, H. Eisen, L.-C. Wen). The rover has 13 temperature sensors; seven are internal and six are external to the warm electronics box. In this experiment, temperature will be monitored during both day and night of each sol to track the thermal characteristics of the vehicle. Analyses of the data may yield information beyond that intended, such as thermal conditions on sunlit or shaded sides of large rocks or the thermal properties of the surface materials. In addition, the temperature measurements, given the distribution on the solar panel, cameras,

and wheels of the rover, will provide estimates of sky, atmosphere, and ground temperatures (respectively), supplementing those measurements taken at the lander for determining atmospheric structure and meteorology.

UHF link effectiveness (L. vanNieuwstadt, H. Stone). The radio signal strength and noise will be monitored as a function of distance between the rover and lander, for various conditions of terrain occlusion and temperature (of the equipment). This experiment will provide measurement of the performance of the radio modems (e.g., bit error rate). There is no obvious scientific benefit from this experiment that we know of at this time.

Vehicle performance (A. Mishkin, H. Stone). In this experiment, all engineering status data will be logged with time tags. These data are collected chiefly to support the other technology experiments, providing measurements of trends and status as part of determining vehicle performance. This includes measurements of solar array power output, voltage and current from the batteries, voltage and current from the power regulation equipment, temperature, data transfer performance (between the rover and lander), inertial sensor and location estimation, and motor performance. During traverses, the rover also measures steering and bogie potentiometers, wheel encoder counts, motor current, hazard/obstacle detection from the camera/laser system, and contact sensor state. Sampling is normally every 10 min during the day and every hour at night. During traverses, the rover samples data every 2 s.

The outputs of this experiment are essential to the other experiments and scientific analyses. In particular, the solar array power output is monitored through three measurements: open cell voltage, shorted circuit cell current, and temperature. These cells and a temperature sensor are mounted on the solar panel and sampled during a given sol. An on-board algorithm estimates the power available from the solar panel, allowing the rover to determine if there is sufficient power available to execute a command. The history of these panel performance measurements and measurements from the rover's material adherence experiment and cameras, can be used in an experiment to measure Mars mass properties. If the rover survives until the first solar eclipse by Phobos in October 1997, the rover measurements can be used along with the lander camera and solar panels on the lander to monitor change in solar flux as a precise function of time during the eclipse. These measurements, along with tracking data for the lander, can be used to constrain the spin pole and tidal dissipation rate of Mars.

Dead reckoning and path reconstruction (L. Matthies, B. Wilcox). The objective of this experiment is to determine the error in the rover on-board position estimator by comparing predicted vehicle positions with positions derived from the dead reckoning sensors (wheel encoders and gyroscope) and with the positions determined by the end-of-sol lander image. The data taken during traverses, in particular, the measurements from the hazard avoidance system, will allow reconstruction of the path traversed by the vehicle as a function of terrain. This experiment may contribute to our understanding of the surface materials by giving estimates of wheel slippage.

Vision sensor performance (L. Matthies, B. Wilcox). Engineering telemetry gathered during traverses is the primary means for the evaluation of the camera and sensor systems used for navigation and hazard avoidance. In support of these engineering measurements, the rover and lander cameras will image the tracks produced by the vehicle in the soil after traverses. These images, taken once per sol, can be correlated with the vehicle telemetry and the reconstructed paths to develop and refine the hazard avoidance and navigation algorithms used on the rover.

Unplanned Opportunities and Natural Situations

The rover can exploit a variety of unplanned opportunities and natural situations. Although it is difficult to anticipate the opportunities and situations in advance, we illustrate five possibilities with Pathfinder and Viking experiences below.

Retraction of the airbags after landing may present unplanned opportunities for the rover. During airbag tests on a simulated Martian surface at the Jet Propulsion Laboratory, some rocks were dragged along the surface and formed small trenches with elevated rims in the cohesionless granular materials of the test bed. A large rock, perhaps one-half meter across, was rotated toward the lander, so that both the originally buried rock and covered soil-like material surfaces were exposed; such surfaces on Mars would have been available for inspection by the rover cameras and analyses with the APXS. Similar-size large rocks that were displaced by the Viking landers had ledges of crust adhering to them [*Moore et al.*, 1987]. Another related opportunity may arise if small rocklets are overturned by the rover wheels, allowing examination of their undersides.

During traverses, the rover will inadvertently create topographic configurations and disturbed materials that are no longer in equilibrium with present-day wind conditions, so that wind erosion will be facilitated. Like the Viking landers, the rover can create such configurations and materials intentionally. Among the Viking configurations were the sample trenches and their elevated tailings and conical piles of disturbed soil-like materials intentionally placed among and atop rocks. After some 1742 sols, winds at the Mutch Memorial Station (MMS or Lander 1) modified and demolished conical piles, leveled tailings rims around trenches, moved centimeter-size clods or rocks, scoured trench walls, and created miniature windtails with orientations unlike those of the preexisting windtails [*Arvidson et al.*, 1983; *Moore*, 1985]. The rover can also excavate similar trenches and construct similar piles of disturbed soil-like materials.

Two miniature landslides on steep slopes of drift material are among the puzzling features that formed at the MMS [*Jones et al.*, 1979]. Little is known about the relief and slopes involved because the first and closest one was hidden to camera 2 by the housing of camera 1 (Figure 11). The second was too far away for estimates [*Moore et al.*, 1987]. For the rover, there are at least two possibilities. First, it could drive to a miniature landslide, if one occurs, orient its cameras, and acquire images to measure the slopes in order to constrain failure conditions. Compositions of both the run-out and scar could be separately determined by the APXS. A second possibility would be to drive to the crest of a small steep slope and initiate a miniature landslide if such favorable slopes are present at the landing site.

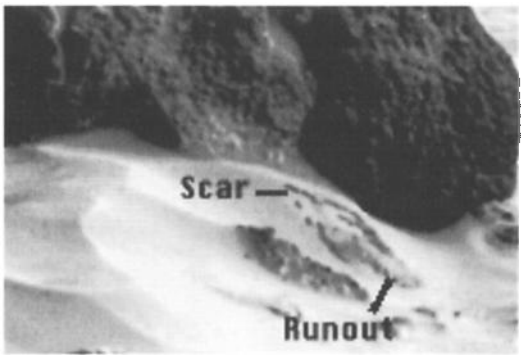

Figure 11. Miniature landslide at base of rock about 8 to 10 m from the MMS. Note scarp, scar, and runout, which span about 0.5 m. Landslide is hidden to camera 2 by camera 1, so that stereoscopic measurements are not possible, but the rover could have positioned itself for stereoscopic image pairs of landslide and placed the APXS for separate analyses of scar and runout (Viking frame 11D095/297).

Another possible active experiment for the rover would help determine if Martian rocks are (or are not) covered with a weathering rind that can be removed or scratched. At a rock with suitable access to the rover wheel cleats, the rover wheels could be rotated while pressed against a surface of the rock. Images by the rover and lander could reveal the effects of the wheels.

If lander camera images indicate a sufficient covering of dust on a ramp magnet that is accessible to the rover after a few weeks of mission operations, the rover could return to the ramp and deploy the APXS sensor head onto the dusty magnet. A comparison of the composition of this dust (especially Ti and Fe) with nearby soil on the ground may help constrain the mineralogy of the magnetic portion of the dust and soil.

Summary

The six-wheeled 10.5-kg Microrover will carry out a wide variety of experiments around the Pathfinder landing site. The primary rover mission is 7 Martian days, and the extended mission is 30 days, but it may continue to operate even longer. Lengths of rover traverses may be only a few meters the first week (nominal speed 0.4 m/min), but could reach tens or even hundreds of meters if it survives longer. A robotic arm attached to the rear of the rover will deploy the alpha proton Xray spectrometer to measure the chemical composition of rocks and soil-like materials. Close-up images of the Martian surface will be taken in stereo with two front monochrome CCD cameras and in color (red, green, infrared) with a single rear CCD camera. From distances of 25 cm, the resolution of rover camera images will be 0.8 mm/pixel, allowing a detailed examination of structures, textures, and fabrics of rocks and soil.

The Rover Team has planned a set of 10 technology experiments to study and assess rover mobility for future exploration of Mars. Results from these experiments are of scientific interest because achievement of some of the goals requires information that parallels that required for scientific goals, some of the results are of direct interest, and some results are required for scientific analyses. The information on types, distributions, and abundances of terrain features required for mobility studies parallels that required for science because types, distributions, and abundances of terrain features are the result of geologic processes. Mechanical properties of soil-like materials, such as friction angle, cohesion, and abrasiveness, are of direct interest because these properties control the responses of the surface to present-day geologic processes. Information on rates of deposition of dusts on the rover would be of direct interest to atmospheric scientists and geologists studying aeolian processes. Rover engineering measurements of temperatures, motor currents, voltages, and so forth will be necessary for some scientific analyses, and other applications may be discovered.

In addition, there will be unplanned opportunities and natural situations that the rover can utilize, such as the investigation of rocks overturned during airbag retraction; monitoring trenches, natural slopes, and piles of soil for slumping or wind erosion; scraping a wheel against a rock; returning to the lander to investigate the dust buildup on a ramp magnet; or climbing to a crater rim for samples and views of distant landforms. The Pathfinder Microrover will be exciting to watch and will return valuable science information as it interacts with the Martian environment, obtains close-up images, and goes exploring.

Acknowledgments. The Rover Team wishes to acknowledge Tony Spear for his guidance and assistance as Pathfinder Project Manager and the help of Sam Arriola (U.S. Geological Survey) for assistance in processing Viking lander images. We thank Tom Chrien and Jose Garcia for characterizing the camera spectral response. Some of the work described was performed at the Jet Propulsion Laboratory, California Institute of Technology, under contract with the National Aeronautics and Space Administration. The constructive reviews of J.G. Taylor and J.W. Salisbury are appreciated. Contributions of H.J. Moore were made as a Scientist Emeritus of the Astrogeology Team of the U.S. Geological Survey.

References

Arvidson, R.E., E.A. Guinness, H.J. Moore, J. Tillman, and S.D. Wall, Three Mars years: Viking Lander 1 imaging observations, *Science*, *222*, 463-468, 1983.

Ballou, E.V., P.C. Wood, T. Wydeven, M.E. Lehwalt, and R.E. Mack, Chemical interpretation of Viking Lander 1 life detection experiment, *Nature*, *271*, 644-645, 1978.

Bickler, D.B., A new family of planetary vehicles, paper presented at International Symposium on Missions, Technologies, and Design of Planetary Mobility Vehicles, CNES, Toulouse, France, 1992.

Binder, A.B., R.E. Arvidson, E.A. Guinness, K.L. Jones, E.C. Morris, T.A. Mutch, D.C. Pieri, and C. Sagan, The geology of the Viking Lander 1 site, *J. Geophys. Res.*, *82*, 4439-4451, 1977.

Blomquist, R.S., The Alpha-Proton-X-ray Spectrometer Deployment Mechanism - An anthropomorphic approach to sensor placement on martian rocks and soil, 29th Aerospace Mechanisms Symposium, *NASA Conf. Publ., CP3293*, 1995.

Carrier, W. D., III, G. R. Olhoeft, and W. Mendell, Physical properties of the lunar surface, in *Lunar Sourcebook*, edited by G. H. Heiken, D.T. Vaniman, and B.M. French, pp. 475-594, Cambridge Univ. Press, New York, 1991.

Christensen, E.M., S.A. Batterson, H.E. Benson, R. Choate, L.D. Jaffe, R.H. Jones, H.Y. Ko, R.L. Spencer, F.B Sperling, and G.H. Sutton, Lunar surface mechanical properties:

Surveyor III Preliminary Report, *NASA Spec. Publ., SP-146*, 94-120, 1967.
Christensen, P.R., and H.J. Moore, The Martian surface layer, in *Mars*, edited by H.H. Kieffer, B.M. Jakosky, C.W. Snyder, and M.S. Matthews, pp. 686-729, Univ. of Ariz. Press, Tucson, 1992.
Clark, B.C., A.K. Baird, R.J. Weldon, D.M. Tsusaki, L. Schnabel, and M.P. Candelaria, Chemical composition of Martian fines, *J. Geophys. Res., 87*, 10,059-10,067, 1982.
Compton, R. R., *Manual of Field Geology*, 378 pp., John Wiley, New York, 1962.
Costes, N.C., W.D. Carrier, J.K. Mitchell, and R.F. Scott, Apollo 11 soil mechanics investigation, chap. 4, Apollo 11 preliminary science report, *NASA Spec. Publ., SP-214*, 85-122, 1969.
Crouch, D.S., Mars Viking surface sampler subsystem, in *Proceedings of the 25th Conference on Remote Systems Technology*, San Francisco, Calif., anniversary issue, pp. 141-152, Am. Nucl. Soc., 1977.
Gisser, K.R.C., M.J. Geselbracht, A. Cappellari, L. Hunsberger, A.B. Ellis, J. Perepezko, and G.C. Lisensky, Nickel-titanium memory metal, *J. Chem. Educ., 71*, 334-340, 1994.
Golombek, M.P., R.A. Cook, H.J. Moore, and T.J. Parker, Selection of the Mars Pathfinder landing site, *J. Geophys. Res.*, this issue.
Hough, B.K., *Basic Soils Engineering*, 513 pp., Ronald Press, New York, 1957.
Jones, K.L., R.E. Arvidson, E.A. Guinness, S.L. Bragg, S.D. Wall, C.E. Carlston, and P.G. Pidek, One Mars year: Viking Lander imaging investigation, *Science, 194*, 1344-1346, 1979.
Lahee, F. H., *Field Geology*, 4th ed., 853 pp., McGraw-Hill, New York, 1941.
Landis, G.A., Dust obscuration of Mars solar arrays, paper IAF-94-R.3.380 presented at 45th Int. Astronaut. Fed. Congr., Jerusalem, Oct. 9-14, 1994.
Landis, G.A., P. Jenkins, J. Flatico, L. Oberle, M. Krasowski, and S. Stevenson, Development of a Mars dust characterization instrument, paper IAF-95-U.4.09 presented at 46th Int. Astronaut. Fed. Congr., Oslo, Norway, Oct. 2-6, 1995.
McKyes, E. and O.S. Ali, The cutting of soil by narrow blades, *J. Terramech., 14*, 43- 58, 1977.
Mitchell, J.K., W.N. Houston, R.F. Scott, N.C. Costes, W.D. Carrier III, and L.G. Bromwell, Mechanical properties of lunar soils: Density, porosity, cohesion, and angle of internal friction, *Geochim. Cosmochim. Acta, 3*, 3235-3253, 1972.
Mittlefehldt, D.W., ALH84001, a cumulate orthopyroxenite member of the martian meteorite clan, *Meteoritics, 29*, 214-221, 1994.
Moore, H. J., The Martian Dust Storm of Sol 1742, *Proc. Lunar Planet. Sci. Conf. 16th*, Part 1, *J. Geophys. Res., 90*, suppl., D163- D174, 1985.
Moore, H.J., and B.M. Jakosky, Viking landing sites, remote sensing observations, and physical properties of Martian surface materials, *Icarus, 81*, 164-184, 1989.
Moore, H.J., G.D. Clow, and R.E. Hutton, A summary of Viking sample trench analyses for angles of internal friction and cohesion, *J. Geophys. Res., 87*, 10,043-10,050, 1982.
Moore, H.J., G.D. Clow, R.E. Hutton, and C.R. Spitzer, Physical properties of the surface materials at the Viking landing sites on Mars, *U.S. Geol. Surv. Prof. Pap. 1389*, 222 pp., 1987.
Morris, E.C., and K.L. Jones, Viking lander 1 on the surface of Mars: Revised location, *Icarus, 44*, 217-222, 1980.
Mutch, T.A., R.E. Arvidson, A.B. Binder, E.A. Guinness, and E.C. Morris, The geology of the Viking 2 Lander site, *J. Geophys. Res., 82*, 4452-4467, 1977.
Oyama, V.I., and B.J. Berdahl, The Viking Gas Exchange Experiment results from Chryse and Utopia surface samples, *J. Geophys. Res., 82*, 4669-4676, 1977.
Rieder, R., H. Wänke, T. Economou, and A. Turkevich, Determination of the chemical composition of Martian soil and rocks: The alpha proton Xray spectrometer, *J. Geophys. Res.*, this issue.
Scott, R.F., W.D. Carrier, N.C. Costes, and J.K. Mitchell, Mechanical properties of the lunar regolith, chap. 10, part C, Apollo 12 preliminary science report, *NASA Spec. Publ., SP-235*, 161-182, 1970.
Seed, H.B., and R.E. Goodman, Earthquake stability of slopes of cohesionless soils, 1, *J. Soil Mech. Div. Am. Soc. Civ. Eng., 90* (SM6), 43-73, 1964.
Sharp, R.P., and M.C. Malin, Surface geology from the Viking landers on Mars: A second look, *Geol. Soc. Am. Bull., 96*, 1398-1412, 1984.
Shoemaker, E.M., E.C. Morris, R.M. Batson, H.E. Holt, K.B. Larson, D.R. Montgomery, J.J. Rennilson, and E.A. Whitaker, 3, Television observations from Surveyor, Surveyor program results, *NASA Spec. Publ., SP 184*, 10-128, 1969.
Terzaghi, K., *Theoretical Soil Mechanics*, 509 pp., John Wiley, New York, 1948.
Treiman, A.H., A petrographic history of martian meteorite ALH84001: Two shocks and an ancient age, *Meteoritics, 30*, 294-302, 1995.

L.W. Avril, R.S. Banes, D.B. Bickler, R.S. Blomquist, G.S. Bolotin, D.F. Braun, D.R. Burger, B.K. Cooper, F. Deligiannis, W.C. Dias, H.J. Eisen, B.H. Fujiwara, R.D. Galletly, G.S. Hickey, K.A. Jewett, E.J. Jorgensen, H.A. Kubo, W.E. Layman, L.H. Matthies, D.P. McQuarie, R.J. Menke, A.H. Mishkin, D.S. Mittman, J.C. Morrison, T.T. Nguyen, D.E. Noon, T.R. Ohm, G.M. Shinn, D.L. Shirley, A.R. Sirota, C.B. Stell, H.W. Stone, L.F. Sword, H.C. Ta, A.D. Thompson, L.M. van Nieuwstadt, M.T. Wallace, L.-C.Wen, B.H. Wilcox, and Y.C. Wu, Jet Propulsion Laboratory, California Institute of Technology, 4800 Oak Grove Drive, Pasadena, CA 91109.

J. Crisp, Mail Stop 241-105, Jet Propulsion Laboratory, California Institute of Technology, 4800 Oak Grove Drive, Pasadena, CA 91109. (e-mail: joy@glassy.jpl.nasa.gov)

D. Ferguson, P. Jenkins, J. Kolecki, G.A. Landis, L. Oberle, and S. Stevenson, NASA Lewis Research Center, Cleveland, OH 44135.

J.R. Matijevic, Mail Stop 230-200, Jet Propulsion Laboratory, California Institute of Technology, 4800 Oak Grove Drive, Pasadena, CA 91109. (e-mail: Jacob.Matijevic@jpl.nasa.gov)

H.J. Moore, U.S. Geological Survey, Mail Stop 975, 345 Middlefield Road, Menlo Park, CA 94025. (e-mail: moore@astmnl.wr.usgs.gov)

(Received March 14, 1996; revised June 5, 1996;
accepted June 14, 1996.)